Reaction and incorporation of H_2 molecules inside single-wall carbon nanotubes through multivacancy defects

Walter Orellana
Departamento de Ciencias Físicas, Universidad Andres Bello, Avenida República 220, 837-0134 Santiago, Chile
(Received 18 July 2009; published 18 August 2009)

The interaction of H_2 molecules with multivacancy defects in single-wall carbon nanotubes (CNTs) and their subsequent incorporation inside are investigated by density-functional theory calculations and molecular dynamic simulations. We examine the stability of multivacancies (nV) in (8,8) CNT, with n the number of missing atoms ($n=2-16$). We find that 16V has the limit size where defect reconstruction is unlikely, preserving the unsaturated border. After hydrogenation, the border is passivated leaving an inert pore of about 6 Å in diameter. We verify that the incorporation and release of H_2 molecules through this nanopore occurs barrierless and its stability in contact with a H_2 gas for both exohedral and endohedral adsorptions is preserved at high temperatures. We also find endohedral binding energies of 0.14–0.21 eV/H_2 at room temperature, which are close to those estimated optimal for a reversible adsorption-desorption process, suggesting that nanoporous CNTs as produced by electron irradiation in a hydrogen atmosphere could be an effective H_2 storage medium, allowing the access to the CNT inner space.

DOI: 10.1103/PhysRevB.80.075421 PACS number(s): 68.43.Bc, 61.46.Fg, 68.43.Fg, 68.43.Mn

I. INTRODUCTION

The materials-science challenge for hydrogen storage can be summarized in the need of a material with large specific surface area where hydrogen can be packed as close as possible together with the reversibility for the uptake and release at nearly ambient conditions. For vehicle applications, the target has been set at 6.5 wt % for stored capacity and 60 kg/m^3 for volumetric density, to be achieved by 2010.[1] Carbon nanostructures have been widely investigated for hydrogen storage due to their comparative low weight and large specific surface area with controversial results. An early experimental work reported that a hydrogen capacity up to 10 wt % could be stored on single-wall carbon nanotubes (SWCNTs) with diameter between 1.6–2.0 nm at room temperature and pressure.[2] However, a later work showed that similar SWCNTs have a hydrogen storage capacity of 4.2 wt % at room temperature and relatively high pressure (10 MPa).[3]

Chemisorption and physisorption are common proposed mechanisms for hydrogen storage in carbon nanostructures. While the former needs the H_2 dissociation follows by the formation of strong C–H bonds,[4] the latter take advantage of the weaker Van der Waals interaction between H_2 and the sp^2 graphitic surface, suitable for reversible adsorption-desorption processes. However, the maximum measured capacity of physisorbed H_2 on SWCNTs is reported on 2 wt %,[5] meanwhile Monte Carlo simulations suggest even lower values (≤ 1 wt %).[6] On the other hand, the driving force for the hydrogen adsorption-desorption process is the difference in chemical potential between the free gas and the adsorbed gas on the CNT, given by $\Delta\mu=\Delta h-T\Delta s$, where Δh and Δs are the changes in specific enthalpy and entropy, respectively, and T is the temperature.[7] The entropic term at room temperature ($T\Delta s$) has been calculated of 0.3–0.4 eV/H_2 for the H_2 adsorption on CNTs of about 1 nm in diameter.[8] Other thermodynamical analyses have found similar results.[7,9] Therefore, the change in enthalpy (or gas binding energy) needs to be of that order to compensate the significant entropic term, allowing the entire adsorption-desorption cycle at ambient conditions. Nevertheless, density-functional theory (DFT) calculations have reported H_2 binding energies of about 0.1 eV at 0 K,[7,10,11] suggesting a very small storage capacity at room temperature.

Irradiation-induced defects in carbon nanostructures is a rapidly evolving area exploring the unique ability of graphitic systems to reconstruct after irradiation.[12] Recent experiments on CNTs have shown that electron beams can focus onto spots of less that 1-nm diameter, displacing an atom or a few of them permanently from its structure,[13] suggesting the creation of controlled nanopores in graphitic materials. In this work we investigate the possibility to increase the hydrogen storage capacity in SWCNTs by introducing nanopores in their walls in order to incorporate H_2 molecules inside. The proposed nanopores are formed by H passivated multivacancy defects which are exposed to molecular hydrogen. The H_2 adsorption and incorporation inside CNTs at finite temperatures is analyzed by *ab initio* molecular dynamic (MD) simulations.

II. THEORETICAL APPROACH

Our DFT calculations were performed with the SIESTA package,[14] which employs norm-conserving pseudopotentials and localized atomic orbitals as basis set (double ζ plus polarization functions in the present work). We use the local-density approximation (LDA) to the exchange-correlation functional,[15] which has shown better results for the physisorption of H_2 molecules on graphene and CNTs than the generalized gradient approximation (GGA).[16] It is found that GGA gives weaker binding energies than LDA.[10,11,17] Whereas, the interaction potential between H_2 and graphene obtained with both DFT-LDA and second-order Møller-Plesset perturbation theory have shown reasonably good agreements,[17,18] suggesting that LDA would be better suited to this kind of calculation. However, in order to obtain an

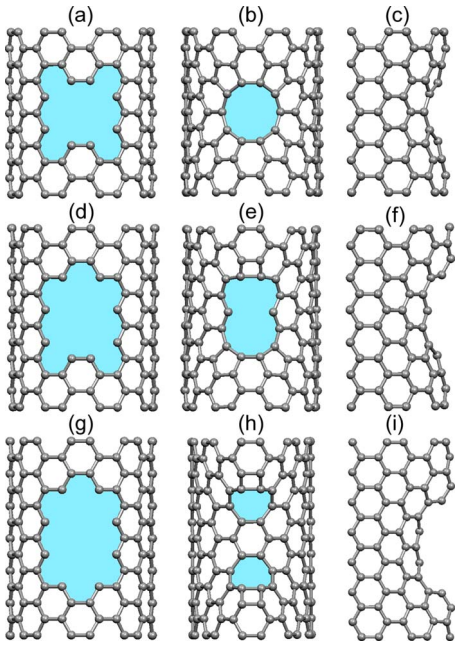

FIG. 1. (Color online) LDA equilibrium geometry of multivacancies in the (8,8) CNT before and after relaxation. (a) Unrelaxed 6V, [(b)–(c)] top and side views of reconstructed 6V. (d) Unrelaxed 8V, [(e)–(f)] top and side views of reconstructed 8V. (g) Unrelaxed 10V, [(h)–(i)] top and side views of reconstructed 10V.

acceptable range for the H_2 adsorption energy on defective CNTs, in the present work most of the calculations are performed considering both LDA and GGA. The armchair (8,8) and (10,10) CNTs with diameters of 11 and 14 Å, respectively, are taken as our model systems to study large-scale vacancy defects. Because of the different vacancy size, we consider supercells with periodic boundary conditions along the tube, containing 5, 6, and 7 CNT unit cells. The lateral separation between CNT images is chosen to be of 10 Å. Four k points were used for the Brillouin-zone sampling for the static calculations and the Γ point for the MD simulations. The H_2 binding energy is calculated as the energy difference between the adsorbed molecules on the CNT and the molecules separate from the CNT using the same supercell. This procedure avoids corrections by bases superposition. The systems were fully relaxed until all forces were less than 0.05 eV/Å. The interaction and stability of the largest vacancy in contact with a H_2 gas of 32 and 64 molecules physisorbed outside and inside the defective CNT is investigated by MD simulations in the grand canonical ensemble using Nosé-thermostat approach[19] at 77, 300, and 600 K over 1 ps.

III. RESULTS AND DISCUSSION

A. Structure and energetic of multivacancies

We first study the energetic and equilibrium geometries of vacancies after removing n atoms from the (8,8) CNT, with $n=2,4,6,8,10,16$, hereafter nV. Our LDA results show that 2V, 4V, and 6V form eight-, nine-, and ten-membered rings, respectively, without undercoordinated atoms at the contour. The formations of these multivacancies are due to the appearance of pentagonal rings (2, 3, and 4 for 2V, 4V, and 6V, respectively). Figure 1 shows the LDA geometries for 6V, 8V, and 10V before and after relaxation. For 8V, we find that two undercoordinated atoms remain, resulting in a 14-membered ring with a square-bond configuration [Fig. 1(e)]. Whereas, the 10V defect repairs by itself forming a smaller CNT section of about 9.5 Å in diameter and 5 Å in length, following a zipperlike mechanism. Its equilibrium geometry shows two eight-membered rings containing two square-bond structures [Fig. 1(h)], which give the needed curvature to reconstruct the defect, similar to pentagonal rings in capped CNTs. It is clear from our results that the sp^2 hybridization is highly favorable in CNTs, which is the driving force behind the self-healing mechanism of multivacancies. The square-bond formation can be seen as a distorted sp^2 structure which becomes energetically more favorable than undercoordinated C atoms. We also find that GGA results for 8V and 10V show different geometries than LDA where some C-C bonds do not form. We find that LDA underestimates the C-C bond length by 0.4%, whereas GGA overestimates it by 0.6%, as compared with the experimental value in diamond. Therefore, the LDA results would give more accurate description of the C-C interaction. Table I compares LDA and GGA multivacancy formation energies. The structure and energetic of 2V and 4V agree well with previous calculations on the (8,8) CNT (Refs. 20–22) and graphene.[12] For 16V we find a LDA formation energy of about 4 eV higher in energy than the GGA, whereas for 2V to 6V it is about 0.4 eV. This large energy difference can also be attributed to the stronger C-C bond resulting from the LDA calculation which tends to reconstruct more firmly extended defects. This is reflected in the area of 16V as obtained with LDA which is about 4% smaller than that obtained with GGA.

TABLE I. LDA and GGA formation energies (E_f) of multivacancies in the (8,8) CNT. N indicates the number of C-C bonds forming the vacancy ring at the equilibrium geometry.

	GGA		LDA	
System	N	E_f (eV)	N	E_f (eV)
2V	8	4.25	8	4.52
4V	9	8.45	9	8.82
6V	10	9.40	10	9.81
8V	16	15.48	14	15.28
10V	18	20.90	8	14.55
16V	26	27.85	26	32.12

B. Hydrogen interaction with multivacancies

Figure 2 shows the equilibrium geometries of 6V and 8V after hydrogenation with five and nine H_2 molecules, respectively. On 6V the molecules have a binding energy of 0.26 eV/H_2, which is 0.14 eV higher than that calculated on a pristine (8,8) CNT. This suggests that the perturbation in the CNT potential-energy surface at the defect site increases

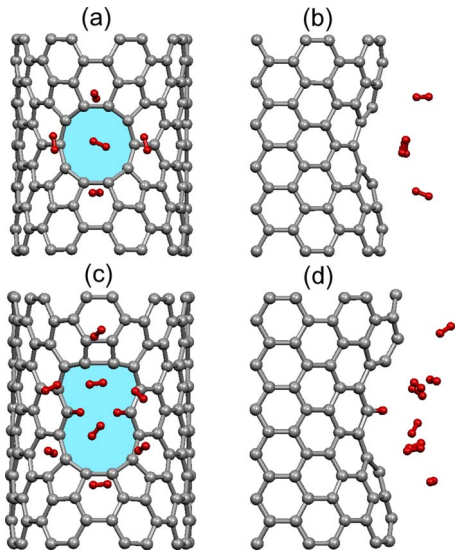

FIG. 2. (Color online) H_2 molecules adsorbed on multivacancies in the (8,8) CNT. [(a)–(b)] Top and side views of five H_2 molecules adsorbed on 6V. [(c)–(d)] Top and side views of eight H_2 molecules adsorbed on the H-saturated 8V (8V-H).

substantially the binding strength of the H_2 molecules. For 8V, the undercoordinated C atoms are passivated by a H_2 molecule which dissociates while approaches to the defect, resulting in a new system, the 8V-H defect. We verify that the dissociative reaction evolves spontaneously with an energy gain of 5.7 eV. The binding energy of the physisorbed molecules onto 8V-H is found to be of 0.22 eV/H_2, whereas the size of the resulting pore is smaller than 6V due to the presence of the C-H bonds [Fig. 2(c)]. The average distance among H_2 molecules on both 6V and 8V-H is about 2.9 Å. Table II lists the physisorption binding energies of a single H_2 molecule onto 2V, 4V, and 10V and five (eight) molecules onto 6V (8V-H). For 2V to 6V we also include GGA results. It is clear that H_2 increases notably its binding strength when adsorbed on the nanopores, which on 6V doubles its value with respect to the adsorption on pristine CNTs. GGA results show the same trend. We also note that the H_2 binding energy on 2V and 10V have almost the same value. This is

TABLE II. Binding energy (E_b) and equilibrium distance (d) from the defect surface of H_2 molecules adsorbed on defective (8,8) CNTs. Results for the H_2 adsorption on the perfect CNT are included.

	GGA		LDA	
System	d (Å)	E_b (eV)	d (Å)	E_b (eV)
(8,8)	3.16	0.076	2.75	0.127
2V	2.84	0.096	2.78	0.186
4V	2.89	0.107	2.66	0.245
6V	3.43	0.102	1.96	0.264
8V-H			2.45	0.217
10V			2.77	0.183

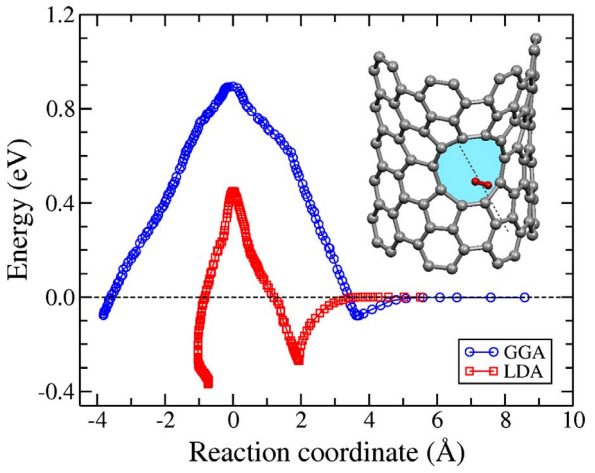

FIG. 3. (Color online) LDA and GGA energy profiles of a H_2 molecule entering inside the (8,8) CNT through a 6V pore of 4.6 Å in diameter. The zero distance is taken at the top of the barriers.

because both vacancies reconstruct forming eight-membered rings.

We now investigate the energy required to incorporate a single H_2 molecule inside the CNT through the 6V pore, the largest one obtained so far. Figure 3 shows our results for the LDA and GGA energy profiles. Here we note the strong differences between both calculations. This result suggests that a more realistic behavior for the H_2 adsorption an incorporation through the 6V pore, of 4.6 Å, might be somewhere between these two curves. Therefore, the molecule has to overcome at least an energy barrier of about 0.5 eV to reach the CNT interior, which would be impractical for storage purposes. The searching for an energetically favorable access to incorporate H_2 molecules inside the CNT led us to consider the larger 16V multivacancy. Because of its size, the defect cannot reconstruct resulting in a 26-membered ring with ten-undercoordinated atoms at the border, as shown in Fig. 4(a). We find that this large vacancy is stable at 0 K. We also verify its stability at an extreme condition of temperature by performing a MD simulation at 600 K during a simulation time of 0.5 ps. After that, we observe the formation of two square-bond structures opposite each other in the vacancy along the CNT, similar to those found in 8V, however the integrity of the CNT is preserved while no further reconstruction is observed. After hydrogenation, the H_2 molecules dissociate while approach to the 16V border forming C-H bonds and leaving an inert H-terminated oval pore (16V-H) with an internal diameter of 6 Å [Fig. 4(b)]. We find that the insertion of a single H_2 molecule through 16V-H occurs barrierless for both LDA and GGA calculations, suggesting the optimal pore size for hydrogen storage.

In order to determine the stability of the pore in a more realistic situation, we put 32 H_2 molecules covering it in a sort of adsorbed gas (exohedral adsorption). Our results at 0 K show that the molecules at the center of the pore tend to enter inside the CNT, stopping just passing the entry. We estimate the gas binding energy subtracting the total energy of the adsorbed molecules the energy of a reference unbound gas, which is calculated by placing the 32 H_2 molecules outside the CNT in positions about 4 Å apart from each other

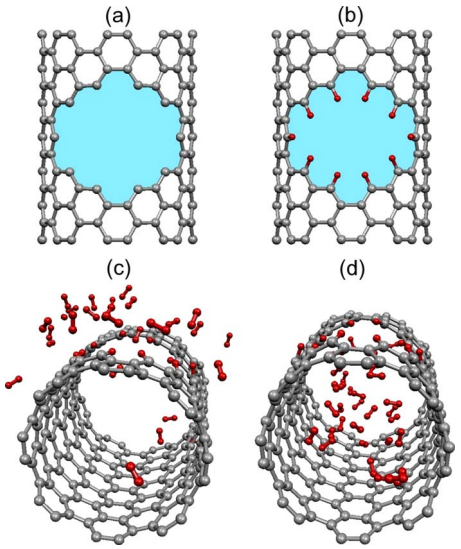

FIG. 4. (Color online) (a) Equilibrium geometry of 16V in a (8,8) CNT forming a 26-membered ring with ten undercoordinated C atoms. (b) Hydrogenate defect forming the 16V-H pore of 6 Å in diameter. [(c) and (d)] Snapshots of 32 H_2 molecules exohedrally and endohedrally adsorbed on the (8,8) CNT with a 16V-H pore at 300 K.

and from the CNT surface in the most diluted concentration possible in our supercell. Thus, the exohedral adsorption energy of the gas is found to be of −0.19 eV/H_2, We also study the same gas adsorbed inside the CNT (endohedral adsorption), after relaxation the molecules arrive to the equilibrium without perturbing the pore. In this case the endohedral adsorption energy is found to be of −0.26 eV/H_2. The above results show an energetic preference for the endohedral adsorption with respect to the exohedral one by 0.06 eV/H_2, favoring the insertion of H_2 molecules inside the CNT. Our model system has a storage capacity ρ_c =2.6 wt % and volumetric density ρ_v=66 kg/m^3.

C. Finite-temperature hydrogen interaction with nanoporous CNTs

To verify the stability of the 16V-H pore and its interaction with the H_2 gas at finite temperature, we perform MD simulations over 1 ps at 77, 300, and 600 K, starting from the equilibrium geometries previously obtained from the exohedral and endohedral adsorptions at 0 K. Comparing the time-average total energies over the simulation time at 77 K, we find an energetic preference for the endohedral adsorption over the exohedral one by 0.22 eV/H_2, suggesting that at low temperatures the H_2 molecules are adsorbed preferentially outside the CNT. However, at 300 and 600 K the endohedral adsorption is the energetically most favorable by 0.06 and 0.10 eV/H_2, respectively. Thus, at room and higher temperatures the H_2 gas would tend to occupy the CNT interior. We also calculate the gas binding energy (or enthalpy) at different temperatures taking the same unbound gas as the reference system, but fixing the center of mass of each H_2 molecule, allowing only vibrational and rotational movements. Our results are listed in Table III. We find that at 77 K

TABLE III. Binding energy (in eV/H_2) of a H_2 gas endohedrally and exohedrally adsorbed on nanoporous CNTs at different temperatures. The (8,8) and (10,10) CNTs with a 16V-H pore are in contact with 32 and 64 H_2 molecules, respectively. Positive binding energies indicate the unbound gas.

System	T (K)	E_b endohedral	E_b exohedral
(8,8):16V-H	0	−0.255	−0.194
	77	0.004	−0.186
	300	−0.136	−0.074
	600	0.095	0.198
(10,10):16V-H	0	−0.249	−0.191
	77	−0.234	−0.181
	300	−0.205	−0.151

the endohedral binding energy is almost zero, which means that the molecules have the same energy of the diluted gas. However, at room temperature this energy increases up to −0.14 eV/H_2, favoring the H_2 endohedral adsorption. Whereas at 600 K, the molecules do not bind the CNT surface. For the exohedral adsorption the behavior is the expected, the binding energy decreases with increasing temperature until the molecules become unbound. Similar results were obtained for a larger (10,10) CNT with a 16V-H pore in contact with a gas of 64 H_2 molecules (ρ_c=4.0 wt %, ρ_v =80 kg/m^3), as shown in Table III. We verify the energetic preference for the endohedral adsorption at 77 and 300 K with larger binding energies of −0.23 and −0.21 eV/H_2, respectively. However, in the (8,8) CNT, the exohedral adsorption is favored at 77 K. These results suggest that the H_2 concentration inside the CNT and the fluctuation of the CNT charge density with temperature play a central role in the endohedral adsorption strength. It is worthy of note that room-temperature endohedral adsorption energies are quite close to those estimated optimal for an entire adsorption-desorption cycle[7,9] and also they agree well with measured values in porous CNTs.[23] Nevertheless, in a previous MD simulation Cheng *et al.* studied the endohedral and exohedral adsorption of three H_2 molecules on a (9,9)-CNT bundle at 77, 300 and 600 K.[24] Although those results agree with ours in the bounded gas at room temperature, they do not match in the strength of the adsorption energy. The extreme diluted gas considered in Ref. 24 may explain such a disagreement.

IV. SUMMARY AND CONCLUSION

We have investigated through *ab initio* calculations the physical properties of large-scale vacancy defects in armchair carbon nanotubes and their interaction with hydrogen molecules at finite temperatures. The aim of this work is to explore nanoporous CNTs as a hydrogen storage medium, with the possibility to access their inner space. The calculations included: (i) the stability and energetic of multivacancies, (ii) The formation of inert nanopores in CNTs with a suitable pore size for the hydrogen incorporation, and (iii) the endohedral and exohedral adsorptions of hydrogen gas on nanoporous CNTs. Our results indicate that multivacan-

cies 2V, 4V, and 6V spontaneously reconstruct leaving perfect pores. The 6V pore size has a diameter of 4.6 Å, however the incorporation of H_2 molecules through it is energetically unlikely. For 8V we find a pore with two undercoordinated C atoms which are saturated by H atoms after the dissociative reaction with a H_2 molecule. Whereas, 10V closes by itself leaving a CNT section with a small diameter. We find that the H_2 binding strength is increased at the nanopore sites due to the perturbation in the CNT potential-energy surface. The interesting case occurs for 16V which due to its large size cannot reconstruct, preserving the unsaturated border. After hydrogenation the border is fully saturated resulting in a pore of about 6 Å in diameter. This nanopore is stable while interacting with a H_2 gas, allowing the barrierless transit of H_2 molecules inside the CNTs. According to our results, the self-healing mechanisms of defective CNTs are the main obstacles for the creation of nanoporous CNTs. However, our results suggest that stable pores could be crated by electron irradiation in a hydrogen atmosphere.

Finally, we studied the endohedral and exohedral adsorptions of H_2 gas on nanoporous CNTs by molecular dynamic simulations. Our results show that at room temperature the endohedral binding strength is higher than the exohedral, suggesting that hydrogen molecules tend to entry through the pores inside the CNT. The endohedral binding energy is find to be of 0.14–0.21 eV/H_2, which are close to those estimated optimal for a reversible adsorption-desorption process at ambient conditions (0.3–0.4 eV/H_2).[7,9] Therefore, nanoporous CNTs could effectively increase the hydrogen-storage capacity with respect to pristine CNTs, allowing the occupation of their inner space.

ACKNOWLEDGMENTS

This work was supported by the Chilean agency FONDECYT under Grant No. 1050197 and by the Anillo Bicentenario under Project No. ACT24/2006.

[1] http://www.eere.energy.gov/hydrogenandfuelcells/
[2] A. C. Dillon, K. M. Jones, T. A. Bekkedahl, C. H. Kiang, D. S. Bethune, and M. J. Heben, Nature (London) **386**, 377 (1997).
[3] C. Liu, Y. Y. Fan, M. Liu, H. T. Cong, H. M. Cheng, and M. S. Dresselhaus, Science **286**, 1127 (1999).
[4] A. Nikitin, H. Ogasawara, D. Mann, R. Denecke, Z. Zhang, H. Dai, K. Cho, and A. Nilsson, Phys. Rev. Lett. **95**, 225507 (2005).
[5] A. Züttel, Mater. Today **6**, 24 (2003).
[6] P. Guay, B. L. Stansfield, and A. Rochefort, Carbon **42**, 2187 (2004).
[7] J. Li, T. Furuta, H. Goto, T. Ohashi, Y. Fujiwara, and S. Yip, J. Chem. Phys. **119**, 2376 (2003).
[8] I. Efremenko and M. Sheintuch, Langmuir **21**, 6282 (2005).
[9] S. K. Bhatia and A. L. Myers, Langmuir **22**, 1688 (2006).
[10] J. S. Arellano, L. M. Molina, A. Rubio, M. J. López, and J. A. Alonso, J. Chem. Phys. **117**, 2281 (2002).
[11] D. Henwood and J. D. Carey, Phys. Rev. B **75**, 245413 (2007).
[12] J. M. Carlsson and M. Scheffler, Phys. Rev. Lett. **96**, 046806 (2006).
[13] A. V. Krasheninnikov and F. Banhart, Nature Mater. **6**, 723 (2007).
[14] J. M. Soler, E. Artacho, J. D. Gale, A. García, J. Junquera, P. Ordejón, and D. Sánchez-Portal, J. Phys.: Condens. Matter **14**, 2745 (2002).
[15] J. P. Perdew and A. Zunger, Phys. Rev. B **23**, 5048 (1981).
[16] J. P. Perdew, K. Burke, and M. Ernzerhof, Phys. Rev. Lett. **77**, 3865 (1996).
[17] Y. Okamoto and Y. Miyamoto, J. Phys. Chem. B **105**, 3470 (2001).
[18] I. Cabria, M. J. López, and J. A. Alonso, Phys. Rev. B **78**, 075415 (2008).
[19] S. Nosé, Mol. Phys. **52**, 255 (1984).
[20] A. V. Krasheninnikov, P. O. Lehtinen, A. S. Foster, and R. M. Nieminen, Chem. Phys. Lett. **418**, 132 (2006).
[21] W. Orellana and P. Fuentealba, Surf. Sci. **600**, 4305 (2006).
[22] R. G. Amorim, A. Fazzio, A. Antonelli, F. D. Novaes, and A. J. R. da Silva, Nano Lett. **7**, 2459 (2007).
[23] M. Shiraishi, T. Takenobu, and M. Ata, Chem. Phys. Lett. **367**, 633 (2003).
[24] H. Cheng, G. P. Pez, and A. C. Cooper, J. Am. Chem. Soc. **123**, 5845 (2001).